On the Existence of Dominant Inter-Area Oscillation Modes in the North American Eastern Interconnect Stability Simulations

Thomas J. Overbye, Sanjana Kunkolienkar, Farnaz Safdarian, Adam B. Birchfield

Dept. of Electrical and Computer Engineering, Texas A&M University, College Station, TX, USA

overbye@tamu.edu, sanjanakunkolienkar@tamu.edu, fsafdarian@tamu.edu, abirchfield@tamu.edu

Abstract—**This paper examines the extent to which distinct inter-area electromechanical modes exist in the North American Eastern Interconnect simulations. Electric grids oscillate, and these oscillations have often been described using the linear systems concept of modes. Furthermore, the inter-area behavior of large-scale grids, such as the North American Eastern Interconnect, is sometimes described using just a few dominant inter-area modes. This paper presents a simulation-based approach to determine the extent to which these modes exist. The approach is motivated using a 2000 bus synthetic grid, and then applied to an 87,000 bus model of the North American Eastern Interconnect (EI). The conclusion is while the EI has common patterns of oscillation, when considering a single operating point for the EI consistent distinct modes are not observed. Rather, the calculated apparent modes appear to be disturbance dependent.**

I. INTRODUCTION

The purpose of this paper is to use a simulation-based approach to study the extent to which specific oscillation patterns exist in large-scale electric grids. Electric grids have dynamics over many different time-scales, with the focus here on dynamics in the time range of electrical cycles out to minutes [1]. Within this time range electric grids oscillate, with the study of these oscillations an area of interest for many years [2], [3]. The portion of the grid affected by the oscillations can vary significantly, ranging from ones within individual generators, to inter-area oscillations that can affect an entire interconnect. The focus of this paper is on these inter-area oscillations, which typically have frequencies of between 0.15 to 1.0 Hz, with a particular consideration of results from North American Eastern Interconnect simulations.

Over the years several techniques for analyzing these oscillations have been developed, with the initial digital computer approaches focused on eigenvalue analysis [4], [5], [6]. This requires linearizing a model of the grid about an operating point. Modes can be determined using the eigenvalues and their associated right eigenvectors, with the eigenvalue providing the mode's frequency and damping, while the eigenvector providing the mode's shape. Of course given that electric grids are nonlinear systems such an approach can never represent the full dynamic behavior of the system, but such modal analysis has certainly been extremely useful. In North America the dominant modes of the grids have been studied for many years, with the modes in the Western Interconnect (WI) particularly well documented. Less work has been done considering modes in the much larger Eastern Interconnect (EI). Some recent references describing these modes include [7]– [15].

The purpose of the paper is to consider the degree to which a small set of dominant modes can be observed in stability simulations of recent models of the EI, building on the results from [16]. Electric grids are nonlinear systems, and they are likely becoming more non-linear, particularly with the growth of inverter-based renewable generation that is often operated at maximum power limits. The models used to represent the grid's behavior are also becoming more nonlinear. For example, with the modeling of deadbands, saturation, nonlinear gain functions, power system stabilizers with limits that can be encountered during disturbances, and many more limits, some of which are binding during normal operation.

The rest of the paper is organized as follows. The next section provides background on the approach used to analyze the EI simulation modes. The third section then provides results from the EI simulations. Conclusions and future directions are in the final section. All calculations and visuali-zations are done with PowerWorld Simulator Version 23.

II. BACKGROUND

To a large extent this paper is motivated by the results from [9] and more specifically from [13]. Using the results from actual frequency disturbances in the EI captured using phasor measurement units (PMUs), both of these papers mention the EI as having two dominant modes. The first is referred to as the Northeast-South (NE-S) mode with a frequency centered on 0.19 Hz. The second is the Northeast-Midwest (NE-MW) mode with a frequency centered near 0.22 Hz. Since [13] is based on four months of continuous tracking, the frequency and damping of each observed mode varied substantially, with the NE-S ranging from 0.15 to 0.22 Hz and the NE-MW ranging between 0.18 and 0.27 Hz. The purpose of this paper isn't to question the results from these papers, but rather to explore the interpretation of the results.

One interpretation is at a particular operating point the EI has two dominant modes, in which each has a specific frequency, damping and shape. Naturally as the grid changes over time, for example with generators and transmission lines changing their statuses, the frequency, damping and shape of these modes would change. An alternative interpretation is the EI actually does not have two, or a small set, of specific dominant modes. Rather, based upon the type of disturbance the EI will oscillate in a nonlinear fashion. Modal analysis can be

used to approximate this oscillation, but the determined modes will be at least somewhat dependent upon the disturbance and will only be able to approximate the grid's nonlinear behavior. With this interpretation there can certainly be general patterns to these oscillations, for example with the edges and more isolated regions of the grid oscillating against the rest. However, these oscillations do not correspond to precise system-wide modes. The premise of this paper is both of these interpretations are consistent with the actual grid measurements from [13], and that a simulation-based approach can help to provide additional insight.

The paper's testing procedure is to apply a variety of different disturbances to the exact same operating point and then use measurement-based ring-down modal analysis to determine the observed modes. Since this is a simulation-based approach, a wide variety of different disturbances can be applied, and all system values are then available for the modal analysis, with the focus here on the bus frequencies. For the disturbances three general different types are used. The first is the outage of one or more large generators. The advantage of this is it matches the events that often cause large frequency disturbances in actual grids. The disadvantage is the generation loss does slightly change the system's operating point. The second type, which can only be done in simulations, is to directly change one or more of the simulation state variables and then allow the grid to ring-down. An example would be discretely changing the frequency at one or more generators. The third type is to induce a forced oscillation, which is done here by either replacing a generator by a time-varying infinite bus in which the frequency of the infinite bus is varied or replacing the power system stabilizer input by a sinusoidal signal. All three disturbance types are used in this paper.

Measurement-based modal analysis is then used to approximate the results for a set of signals using a set of exponentially scaled sinusoidals. That is, given a time-varying signal, $y_j(t)$, the goal is to obtain a reconstructed signal, $\hat{y}_j(t)$, such that,

$$\hat{y}_j(t) = d_j(t) + \sum_{i=1}^{M} A_{j,i} e^{\sigma_i t} \cos(\omega_i t + \phi_{j,i}) \tag{1}$$

where M is the number of modes, $d_j(t)$ is a usually linear detrending term, σ_i is the damping factor, ω_i is the frequency, $A_{j,i}$ is the amplitude, and $\phi_{j,i}$ the phase. When multiple signals are considered, all of the signals share the same set of frequencies and damping, albeit with different amplitudes and phases. The percent damping for the ith mode, D_i, is defined as

$$D_i = \frac{-\sigma_i}{\sqrt{\sigma_i^2 + \omega_i^2}} \times 100 \tag{2}$$

There are a number of different methods that could be used to determine the parameters of (1), all of which work by uniformly sampling the signals over a period of time. A number of different metrics can then be used to quantify the error between the original and reconstructed signals, with the average error approach used here,

$$E_j = \frac{1}{N} \sum_{k=1}^{N} \left| y_j(t_k) - \hat{y}_j(t_k) \right| \tag{3}$$

where E_j is the average error for signal j, N is the number of samples, and t_k is the kth sample time.

Since the goal here is to analyze a potentially large number of bus frequency signals, this paper utilizes the Iterative Matrix Pencil Method (IMP) [17], which provides a computa-tionally tractable extension of the Matrix Pencil Method (MPM) [18] to large sets of signals, to determine the parameters of (1). With the IMP results, and the computation insight from [19], how each signal participates in each calculated mode can be readily determined to give a calculated mode shape. The mode shapes can then be visualized using the techniques presented in [20], [21], [22]. If the grid actually has distinct modes, then the IMP calculated modes should be consistent in frequency, damping and shape between the disturbances.

Before moving on to the EI, this approach is illustrated using a fully public 2000 bus (2K), 60 Hz, synthetic grid with 544 generators that covers a geographic footprint of most of the U.S. state of Texas using 500/230/161/115 kV transmission system. Details on the creation of this grid are given in [23], [24], and [25]; the full grid model is available at [26], and some initial modal results are provided in [16]. The oneline for this case is shown in Figure 1, with the transmission lines colored based on their nominal voltage (orange for 500 kV, purple for 230 kV, and black for lower voltages), and with the green ovals showing the location of the generators. The location of the key buses mentioned in this paper are also shown. For the scenarios presented here the total load is about 67 GW.
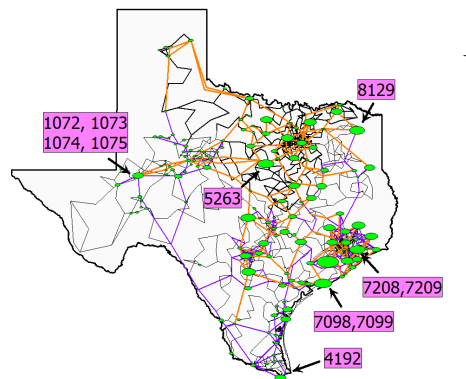

Figure 1: Texas 2000 Bus System Oneline

The paper's procedure for determining the existence of modes is to apply a set of disturbances to the same operating point to see whether consistent results observed. If the observed mode's frequency, damping or shape changes substantially based on the disturbance, then it is reasonable to question whether the mode exists, or whether the nonlinear electric grid is exhibiting a more complex type of behavior. For both the 2K and the EI grid the results are determined using time domain simulation with a time step of 0.5 cycles.

The first 2K disturbance is opening the 1239 MW generator at bus 7098 at a simulation time of 1.0 seconds. In order to show

the overall bus frequency behavior, Figure 2 plots the frequency signals for all 2000 buses, while Figure 3 shows just the buses highlighted in Figure 1. In order to determine the modes using the IMP, a time period and sampling rate needs to be selected. Since the modes of interest are typically less than 5 Hz and the computational complexity of the IMP varies with the cube of the number of samples, the results are sampled at 10 Hz (ten per second). In general increasing the sampling rate above this value does not substantially change the results. For the sampling time period, a rule of thumb is to start sampling slightly after the disturbance has occurred, and then to continue until most of the dynamics have damped out. The results are somewhat dependent on the sampling time period [27]; here a time period of between 2 and 14 seconds is used. For this disturbance the modal results with frequencies between 0.2 and 1.0 Hz for the above time period are given in Table 1.
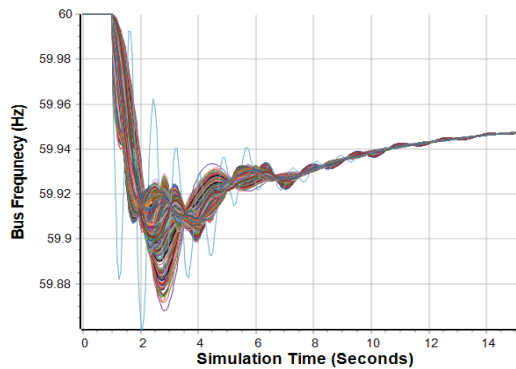
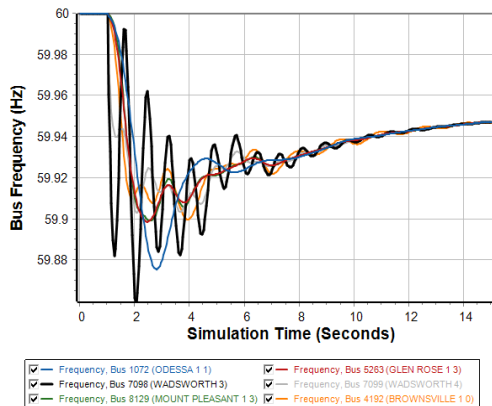Figure 2: All 2K Grid Bus Frequencies for Bus 7099 Generator Outage

Figure 3: 2K Frequencies for Buses 1072, 4192, 5263, 7098, 7099, 8129

Table 1: Modal Frequency and Damping for the Figure 2 Signals

Freq (Hz)	Damping (%)	Average Magnitude (Hz)
0.21	33.6	0.020
0.36	22.6	0.015
0.63	6.7	0.004
0.73	17.5	0.004
0.97	8.5	0.004

From this anaylsis since the modal information for each signal is now known, reconstructed signals can be determined using (1). These reconstructed signals are shown in Figure 4, noting that the x-axis time period is now the sampling time period, from 2 to 14 seconds. The average error for each signal

can be determined using (3), with the result being a fairly close match. The average error over all buses is 0.00025 Hz, with Bus 1051 having the highest average error of 0.0007 Hz. A comparison between the Bus 1051 original and recon-structed signals is given in Figure 5. While the average error appears low, it does need to be weighed against the relatively low magnitudes of the modes from the table. The spatial variation in the total bus error is contoured in Figure 6 in which locations of higher error indicate a potentially more nonlinear response. The key takeaways are the IMP has done a good job of quantifying this response into modes, and the results can now be used to compare different disturbances.
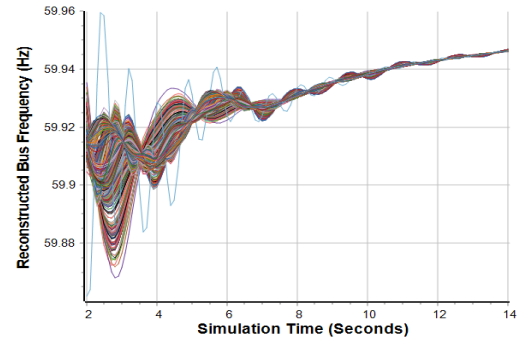

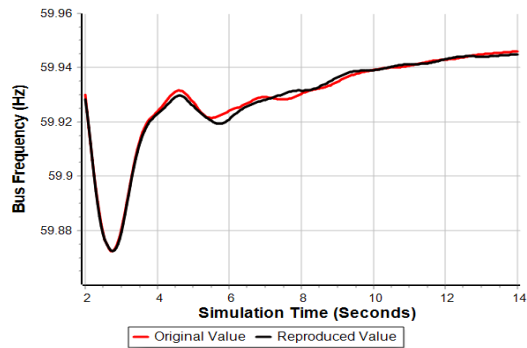Figure 4: 2K Reconstructed Frequencies for All Buses

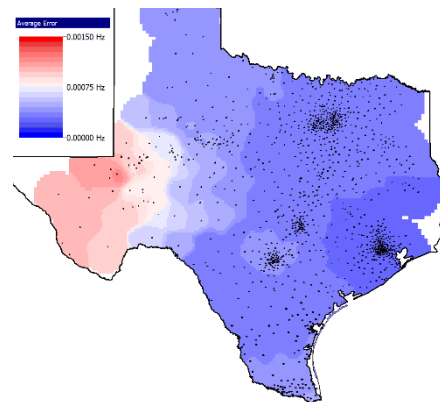Figure 5: Results from Bus with the Highest Average Error (Bus 1051)

Figure 6: Spatial Variation in Bus Average Frequency Error

A key method in which the results will be used to compare disturbances is by visualizing the mode shapes using the techniques presented in [28], and [29]. If the grid actually has

distinct modes and the disturbance actually excites the mode, then the IMP calculated modes, including their shapes, should be consistent between disturbances. For example, Figure 7 visualizes the shape of the 0.36 Hz mode from Table 1 in which the arrows show the magnitude and angle of the mode at different locations. That is, for the ith mode, the figure is showing the $A_{i,j}$ and $\phi_{i,j}$ values from (1). In the figure the length of the arrows is proportional to their magnitudes, with the values normalized so the largest component has a value of 1.0. The arrow thickness also increases slightly with magnitude. The arrow direction indicates the phase angles. While the actual angle is needed in doing the reconstructions, from a visualization perspective all that is needed is the relative phase angles. Hence all the angles can be shifted as desired. For consistency in all the 2K grid mode visualizations the angles are shifted so the arrow at Bus 4192 (in far South Texas) points to the east (right). Also, to aid with the visualize the figure has been decluttered, so rather than showing arrows for all 2000 bus values a much smaller number are actually visualized. Finally, a color contour utilizing a perceptually uniform circular color mapping [30], [31] is used to visualize the angles. The figure indicates that at least for this disturbance the western part of the grid tends to oscillate against the southern and to some extent eastern portions of the grid. This pattern will be called the West Mode.
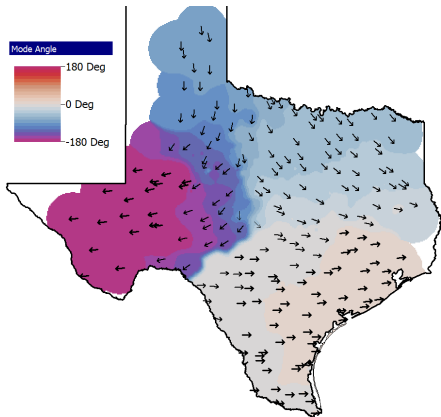

Figure 7: Visualization of 0.37 Hz West Mode with 21.7% Damping

With this approach the other modes from Table 1 could also be visualized. The 0.21 Hz mode is not particularly interesting since all the arrows are pointing to the left and the mode has high damping. The 0.63 Hz mode, shown in Figure 8, is Southeast Texas oscillating against the rest of the grid (Southeast Mode). The presence of this mode is not surprising since in the 2K grid Southeast Texas has a large amount of load and generation that has a fairly weak interconnection with the rest of the system. The 0.73 Hz mode is the south and west oscillating again the north (South Mode), while the 0.95 Hz mode is central region oscillating again the rest of the grid.

The consistency of the modes can then be assessed by repeating this process with different disturbances. For example, changing the disturbance from outaging the 1239 MW generator at Bus 7098 to also outaging the 1350 MW generator at Bus 7099, results the Table 2 modes. Overall the grid shows

the same modes, albeit with somewhat changed frequencies and damping, and higher magnitude values due to a doubling of the MWs lost in the disturbance. The average error between the actual and reconstructed signals increased from 0.00025 Hz to 0.00037 Hz. Redoing the visualizations shows that the mode shapes remain relatively consistent.
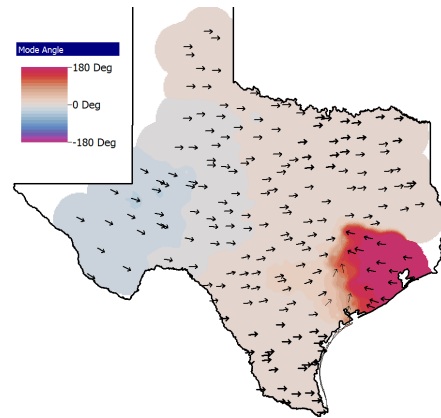

Figure 8: Visualization of 0.63 Hz Southeast Mode

Table 2: Modal Frequency and Damping for Bus 7098, 7099 Outage

Freq (Hz)	Damping (%)	Average Magnitude (Hz)
0.23	46.5	0.063
0.40	21.7	0.037
0.63	5.6	0.006
0.70	8.7	0.006
0.95	7.6	0.007

The next portion of this example considers changing the disturbance type from opening generators to the second type of just changing the states values. Here the disturbance consists of just dropping the frequencies of the Buses 7098, 7099 generators by 0.5 Hz. This gives similar results for the West Mode (now 0.35 Hz with 24.5% damping). There are changes in the Southeast Mode (shown in Figure 9 with 0.66 Hz and 7.1% damping) and the South Mode, which now is at 0.63 Hz with 11.5% damping. However, this could be due to the previous disturbance type of opening generators was altering the operating point.
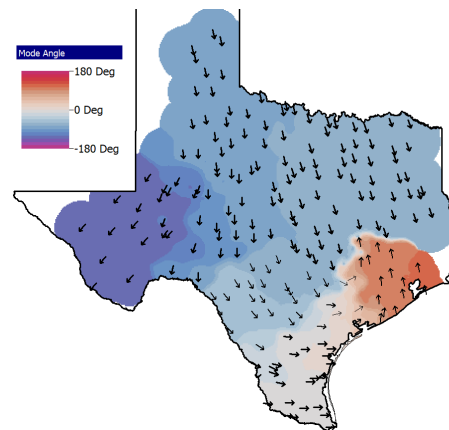

Figure 9: Visualization of 0.66 Southeast Mode with 7.1% Damping

The last disturbance type is to induce a forced oscillation. There are several ways this could be accomplished. One

approach that is used with the actual grid to determine the frequency response is to use probing tests [32]. Motivated by this, a simulation approach used here is to replace the power system stabilizers at one or more generators by a sinusoidal voltage magnitude injection at a specified frequency. Another approach used here is to replace a generator(s) by a time-varying infinite bus in which its voltage frequency and/or magnitude is varied. As an example, Figure 10 shows the 2K bus frequencies when a 0.37 Hz forced oscillation is induced at Buses 1072 to 1075 using the infinite bus approach. As before the IMP can be used to determine the modes, which will naturally be dominated by an undamped one at the forcing frequency of 0.37 Hz. While this approach cannot show the mode's damping, it can provide an approximation of its shape. This is shown in Figure 11. In comparing Figure 7 with Figure 11 there is a clear similarity in the pattern of oscillation (West Texas versus the rest), but the patterns are far from identical. Figure 12 shows a visualization of the mode induced by replacing the Bus 7208 stabilizer with a 0.64 Hz, 0.1 per unit voltage magnitude injection, with the resultant shape quite close to the one in Figure 8.
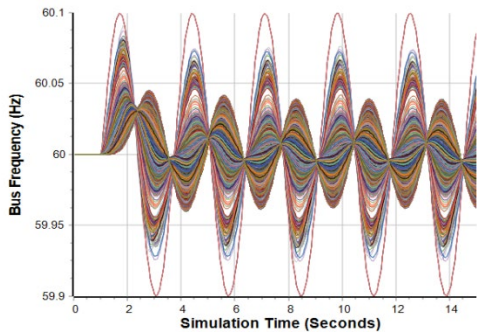

Figure 10: 2K Bus Frequencies for Buses 1072-1075 Forced Oscillation
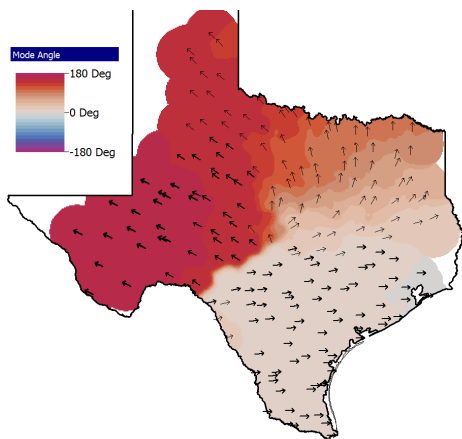

Figure 11: Visualization of 0.37 Hz Mode from the Forced Oscillation

In preparing this paper a large number of different disturbances have been considered using this approach. The conclusion is at least for this operating condition, the 2K grid does have several strong patterns of oscillation. However, for each the frequency, damping and shape does vary based upon the type of disturbance. The next section applies this same approach to an EI model.
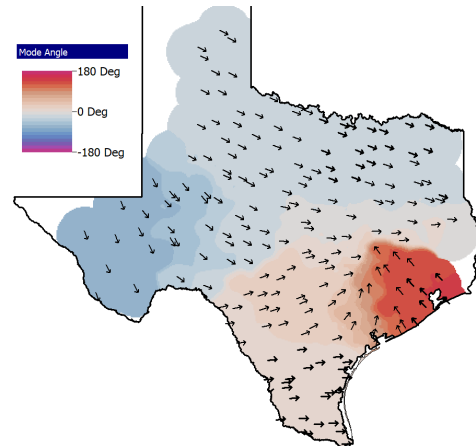

Figure 12: Visualization of 0.64 Hz Mode from a Forced Oscillation

III. NORTH AMERICAN EASTERN INTERCONNECT (EI) RESULTS

Building on the foundation provided with the 2K example, this section provides results from simulations using an 87,000 bus, 9500 generator, 130 area EI model. To facilitate the same visualization done with the 2K grid, almost all the buses have been placed into about 35,000 electric substations with almost all these substations having known geographic locations. For the stability simulations the EI grid has 150 separate model types, 18,000 model instances, and about 104,000 state variables. This model has two large electric islands, with largest containing all most all the buses (85,500), and the second the 1300 bus Quebec Interconnection that operates asynchronous from the main island. There are also several smaller islands with the largest representing part of Manitoba. All of the applied disturbances only impacted the main island. To provide an overview of the location of the generation, Figure 13 provides a geographic data view (GDV) [33], [34] visualization with the generation for each area shown using a rectangle whose area is proportional to the generation and whose color indicates the amount of area exports (red) or imports (blue).
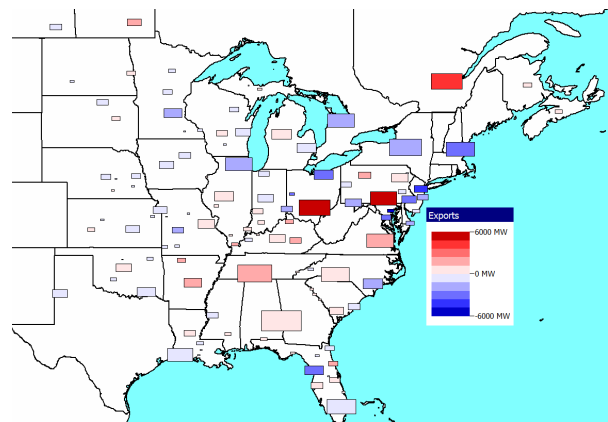

Figure 13: Geographic Data View (GDVs) for EI Area Generation

As with the 2K grid, the existence of unique modes can be studied by applied a variety of different disturbances to the EI

model for the same operating point, and then calculating the modes as it rings down. The operating point considered here corresponds to estimated Summer Peak conditions. A particular focus is on the previously mentioned NE-S and NE-MW modes from [13]. Since both modes involve the Northeast, the first disturbance considered is the outage of a large generator in the US New England region (NEng). As with the 2K case, the simulations are run for a total of 15 seconds using a 0.5 cycle time step, with the disturbance applied at 1.0 seconds. Figure 14 shows the bus frequency signals for all 87,000 buses, again with the intent of the figure obviously not to show the response at any particular bus but rather the overall pattern.
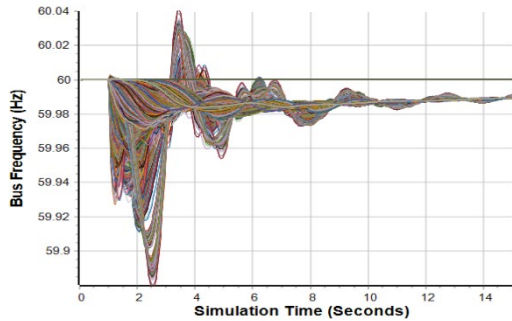

Figure 14: EI Frequency Response for a New England Generator Outage
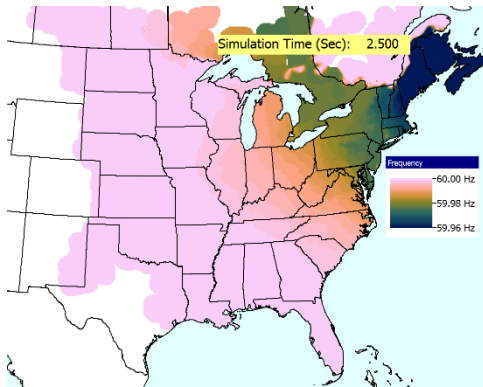

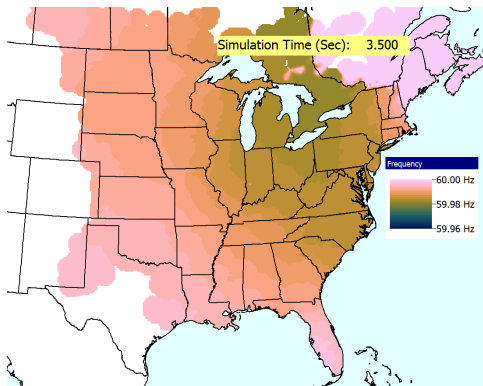Figure 15: Spatial Frequency for the Figure 14 Scenario at 2.5 Seconds

Figure 16: Spatial Frequency for the Figure 14 Scenario at 3.5 Seconds

At any point in the simulation the spatial variation in the frequencies could also be visualized, with Figure 15 showing the results at 2.5 seconds using the contouring approach of [35] and Figure 16 at 3.5 seconds. Note that the disturbance

propagates out from the outage location, with some fundamentals of such propagation given in [36], and EI propagation speed estimates given in [37]. As noted in [28], movies can be made uses a series of such images.

Table 3 shows the key calculated modes for this example, again sampling at 10 times per second with a time period of between 2.0 and 14.0 seconds. Using the previous approach, the shape of each mode could be visualized, with the 0.27 Hz one shown in Figure 17. Again, to aid in comparison, the magnitude of all the values is normalized so the largest value is 1.0. The angles are also set to use a consistent reference direction, arbitrarily set so a bus in NEng always points right (east). The issue is again the degree to which the observed modes vary with the disturbance, and also how well the results match those from [13].

Table 3: Modal Frequency and Damping for the Figure 14 Bus Frequencies

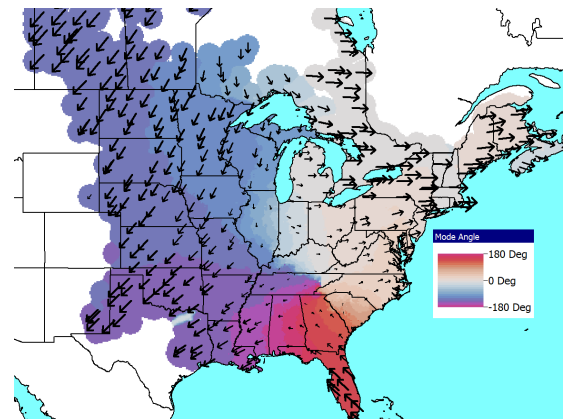| Freq (Hz)	Damping (%)	Average Magnitude (Hz)
0.27	21.3	0.0087
0.34	14.0	0.0063
0.56	7.5	0.0020
0.66	12.8	0.0023
0.83	5.3	0.0007

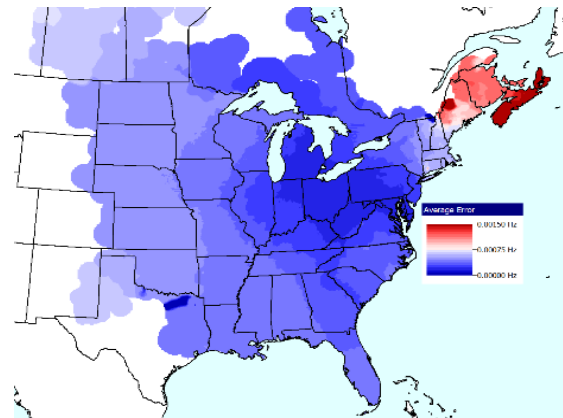Figure 17: NEng Scenario, 0.27 Hz Mode Shape, 21.3% Damping

Figure 18: Spatial Variation in Bus Average Frequency Error

The results from Figure 17 indicate the Northeast (NE) oscillating against the West and to some extent against the US state of Florida. This is similar to the NE-MW Mode from [13] with its frequency and damping within the reported ranges. Again the accuracy of the IMP can be determined by using (3)

to calculate an average error for each bus. Averaging over all buses, the average frequency error is 0.00036 Hz, with a high value of 0.0021 Hz. Again, while this value is relatively low, it does need to be weighed against the relatively small magnitudes of the modes in Table 3. The spatial variation in this error is shown in Figure 18 with the highest errors in the far Northeast, a region that actually has very few buses. Figure 19 compares the original and reconstructed signals for the bus with the highest average error. The conclusion is that the IMP appears to again be doing a fairly good job of reconstructing the overall system frequency response, however there is certainly error due in part to the nonlinear system response.
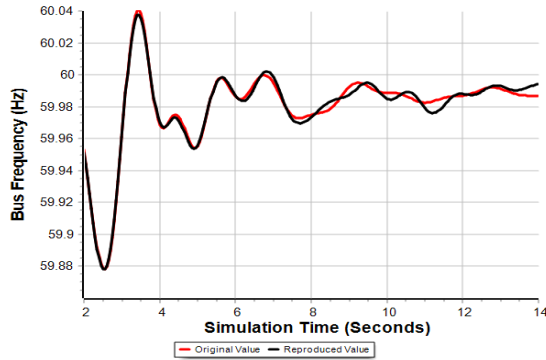

Figure 19: Comparison for Bus with the Highest Average Error

The next step is to sequentially apply a variety of other disturbances to the sane operating point to see if similar modes are observed. As a second test looking for the NE-MW mode, the disturbance simulated is the outage of a large generator in the US state of Nebraska. Figure 20 shows the 0.25 Hz mode, which has calculated 20.2% damping and an average magnitude of 0.0057 Hz. In comparing this figure with Figure 17 there is a broad similarity of the NE oscillating against the west, but also some substantial differences.
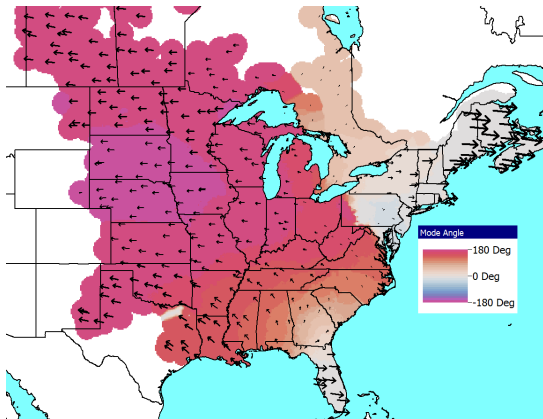

Figure 20: Nebraska Scenario, 0.25 Hz Mode Shape, 20.2% Damping

To test to see if the NE-S Mode is observed, the next disturbance is the outage of a large generator in the US state of Mississippi that should excite this mode. A 0.25 Hz mode with 23.5% damping is observed, but as shown in Figure 21 it seems to consist mostly of the northwest region oscillating against the NE and to some extent Florida. Since in all of these results

Florida seems to oscillate separately, the next scenario is a generator outage there. A 0.23 Hz mode with 21.5% damping is observed, with its shape shown in Figure 22.
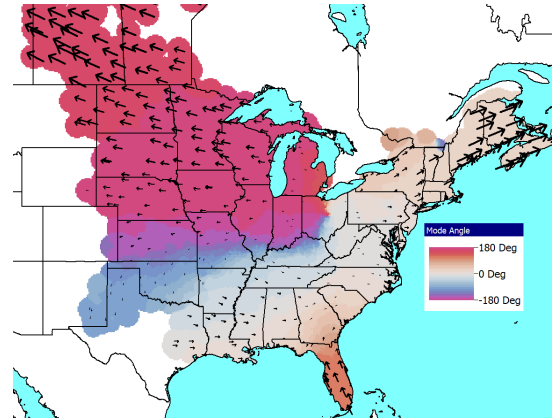

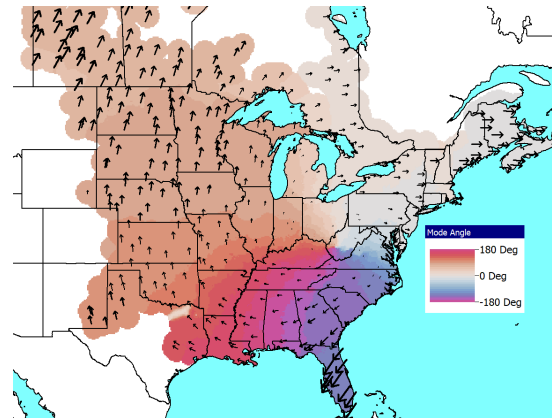Figure 21: Mississippi Scenario, 0.25 Hz Mode Shape, 23.5% Damping

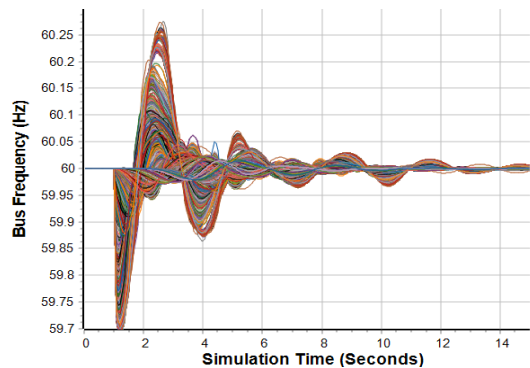Figure 22: Florida Scenario, 0.23 Hz Mode Shape, 21.5% Damping

Figure 23: Northeast Frequency Change Scenario

To avoid having the disturbance modify the operating point, the next scenario consists of decreasing the speed at all the generators in NEng and the three far eastern Canadian provinces by 0.3 Hz at a time of 1.0 seconds, and then letting the grid ringdown   . Figure 23 shows the frequency response for this disturbance at all the buses. In applying the IMP to this scenario, the two largest modes in the response are one at 0.22 Hz with 27.1% damping and another slightly larger one at 0.35

Hz with 15.0% damping. Their mode shapes are shown in Figure 24 and Figure 25 respectively.
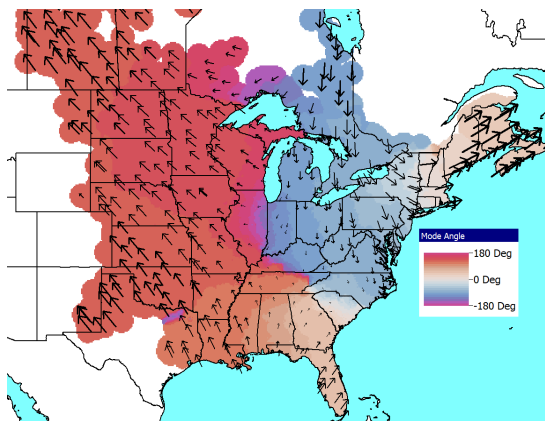

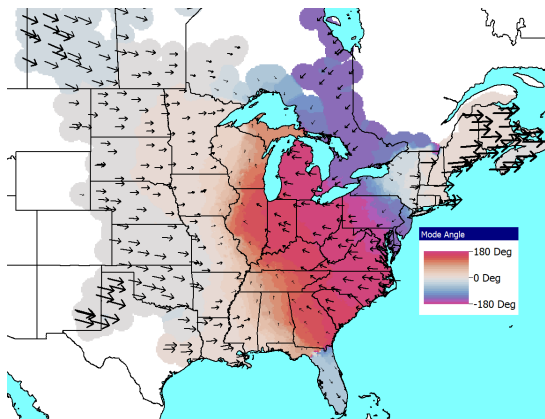Figure 24: Northeast Disturbance, 0.22 Hz Mode Shape, 27.1% Damping

Figure 25: Northeast Disturbance, 0.35 Hz Mode Shape, 15.0% Damping

Excepting Figure 25, a commonality in all of these results is an oscillation with a frequency in the range of 0.21 to 0.27 Hz and damping of between 20 and 27%. However, the shape of this oscillation is strongly dependent upon the disturbance. To get more insight into the shape, the next disturbance is a 0.27 Hz forced oscillation applied at the previously used NEng generator. The resultant system frequencies are shown in Figure 26, while the calculated mode shape is visualized in Figure 27. The results are somewhat similar to the NEng generator contingency, but again they have some important differences.

IV. CONCLUSION AND FUTURE DIRECTIONS

This paper has provided a simulation-based methodology for examining the modal behavior in large-scale electric grids, with a focus on the EI. A conclusion is that the IMP can be used both to fairly effectively represent the frequency response at all the buses in terms of a small number of modes and to quantify the errors associated with this approach. Based on results for the two grids considered, while the systems show consistent general patterns of oscillation frequencies and to some extent damping, when the same operating point is subjected to different disturbances, consistent mode shapes are not observed, particularly for the EI. Another conclusion is that simulations with visualization can play a helpful role in understanding the nature of these oscillations. A final conclusion and future direction is the need for additional research in this area.
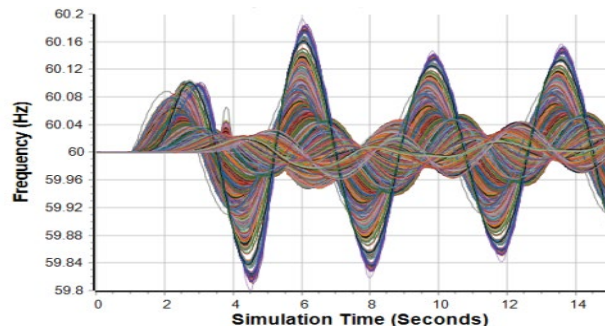

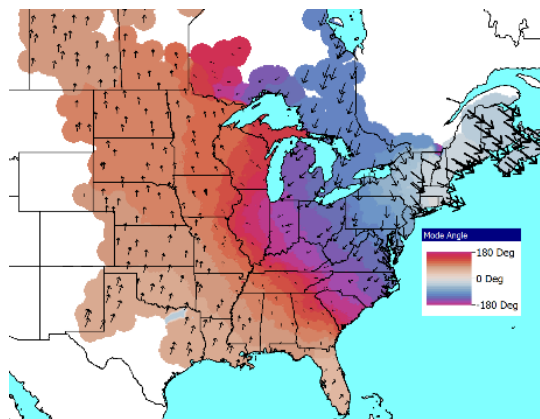Figure 26: Frequencies of 0.27 NEng Forced Oscillation

Figure 27: NEng Forced Oscillation 0.27 Hz Mode Shape

To facilitate this research, another future direction this is further development of high quality, large-scale synthetic grids that can be made publicly available with dynamic models that mimic the complexity of those found in actual grids such as the EI. While this paper did study the EI, the model details needed for others to replicate these results cannot be made generally available since these detailed parameters are considered to be critical energy/electricity infrastructure information [38]. The 2K grid is public, as are some other larger grids that have at least some dynamics [26]. However currently these grids do not have nearly the complexity of the dynamics included in the actual grids, and they often lack the amount of wind and solar generation present in the actual grids. With such grids, the modal behavior presented here can be better studied using a replicable manner.

V. ACKOWLEDGEMENTS

REFERENCES

[1] P.W. Sauer, M.A. Pai, J.H. Chow, *Power System Dynamics and Stability*, John Wiley & Sons Ltd., Hoboken, NJ, 2018.

[2] C. Concordia, S. B. Crary, J.M. Lyons, Stability Characteristics of Turbine Generators, *AIEE Transactions*, vol. 57, pp. 732-744, 1938.

[3] F.R. Schleif, J.H. White, "Damping for the Northwest – Southwest Tieline Oscillations – An Analog Study," *IEEE Trans. Power App. & Syst*., vol. PAS-85, pp. 1239-1247, December 1966.

[4] R.T. Byerly, R.J Bennon, D.E. Sherman, "Eigenvalue Analysis of Synchronizing Power Flow Oscillations in Large Electric Power Systems, *IEEE Trans. Power App. & Syst*., vol. PAS-101, pp. 235-243, Jan. 1982.

[5] P. Kundur, G.J. Rogers, D.Y. Wong, L. Wang, M.G. Lauby, "A Comprehensive Computer Program Package for Small Signal Stability Analysis of Power Systems," *IEEE Trans. Power Sys.*, vol. 5, pp. 1076-1083, Nov. 1990.

[6] P. Kundur, *Power System Stability and Control*, McGraw-Hill, Inc., New York, NY, 1994.

[7] Z. Yuan, T. Xia, Y. Zhang, L. Chen, P. N. Markham, R. M. Gardner, and Y. Liu, "Inter-Area Oscillation Analysis Using Wide Area Voltage Angle Measurements from FNET," IEEE PES General Meeting, Minneapolis, MN, July 2010.

[8] K. Zhang, Y. Ye, L. Chen, Y. Zhang, R. M. Gardner, Y. Liu, "FNET Observations of Low Frequency Oscillations in the Eastern Interconnection and Their Correlation with System Events," IEEE PES General Meeting, Detroit, MI, July 2011.

[9] *Interconnection Oscillation Analysis*, North American Electric Reliability Corporation (NERC), Atlanta, GA, July 2019.

[10] J. Follum, T. Becejac, R. Huang, "Estimation of Electromechanical Modes of Oscillation in the Eastern Interconnection from Ambient PMU Data," 2021 IEEE Power & Energy Society Innovative Smart Grid Technologies Conference, Washington, DC, USA, Feb. 2021.

[11] *Modes of Inter-Area Oscillations in the Western Interconnection*, Western Interconnection Modes Review Group, WECC, 2021.

[12] R.T. Elliott, D.A. Schoenwald, "Visualizing the Inter-Area Modes of the Western Interconnection," IEEE PES 2022 General Meeting, Denver, CO, July 2022.

[13] J. Follum, N. Nayak, J. Eto, "Online Tracking of Two Dominant Inter-Area Modes of Oscillation in the Eastern Interconnect," 56th Hawaii International Conference on System Sciences, Lahaina, HI, Jan. 2023.

[14] *Recommended Oscillation Analysis for Monitoring and Mitigation Reference Document*, North American Electric Reliability Corporation (NERC), Atlanta, GA, Nov. 2021.

[15] S. Biswas, Q. Nguyen, X. Lyu, X. Fan, W. Du, Z. Huang, "Evaluating the Impact of Retiring Synchronous Fossil Fuel Generators on Inter-Area Oscillations in the U.S. Western Interconnection, 57th Hawaii International Conference on System Sciences, Honolulu, HI, Jan 2024.

[16] T.J. Overbye, S. Kunkolienkar, "On the Existence of Distinct Inter-Area Electro-Mechanical Modes in North American Electric Grids," Kansas Power and Energy Conference, Manhattan, KS, April 2023.

[17] W.C. Trinh, K.S. Shetye, I. Idehen, T.J. Overbye, "Iterative Matrix Pencil Method for Power System Modal Analysis," 52nd Hawaii International Conference on System Sciences, Waikoloa, HI, Jan 2019.

[18] M.L. Crow, A. Singh, "The Matrix Pencil for Power System Modal Extraction," *IEEE Trans. Power Systems*, vol. 20, pp. 501-502, Feb. 2005.

[19] A.R. Borden, B.C. Lesieutre, J. Gronquist, "Power System Model Analysis Tool Developed for Industry Use," Proc. 2013 North American Power Symposium, Manhattan, KS, Sept. 2013.

[20] I. Idehen, B. Wang, K.S. Shetye, T.J Overbye, J.D. Weber, "Visualization of Large-Scale Electric Grid Oscillation Modes," 50th North American Power Symposium, Fargo, ND, September 2018.

[21] T.J. Overbye, K.S. Shetye, J. Wert, W. Trinh, A. Birchfield, T. Rolstad, J.D. Weber, "Techniques for Maintaining Situational Awareness During Large-Scale Electric Grid Simulations," 2021 Power and Energy Conference at Illinois, Champaign, IL, April 2021.

[22] W. Trinh, S. Kunkolienkar, Y. Liu, and T. J. Overbye, "On the Sensitivity of Ring-Down Observed Inter-Area Modes in Large-Scale Electric Grids Using a Simulation Approach," IEEE. Power and Energy Conference at Illinois (PECI), Champaign, IL, March 2022.

[23] A.B. Birchfield, T. Xu, K. Gegner, K.S. Shetye, T.J. Overbye, "Grid Structural Characteristics as Validation Criteria for Synthetic Networks," *IEEE Trans. Power Syst.*, vol. 32, pp. 3258-3265, July 2017.

[24] T. Xu, A.B. Birchfield, K.S. Shetye, T.J. Overbye, "Creation of Synthetic Electric Grid Models for Transient Stability Studies," *10th Bulk Power Sys. Dynamics & Control Symposium*, Espinho, Portugal, Sept. 2017.

[25] T. Xu, A. B. Birchfield, and T. J. Overbye, "Modeling, Tuning, and Validating System Dynamics in Synthetic Electric Grids," *IEEE Trans. on Power Systems*, vol. 33, no. 6, pp. 6501–6509, Nov. 2018.

[26] Texas A&M University Electric Grid Test Case Repository, electricgrids.engr.tamu.edu/

[27] W. Trinh and T.J. Overbye, "Sensitivity of Modes from Modal Analysis of Electric Grids," Kansas Power and Energy Conference, Manhattan KS, April 2021.

[28] I. Idehen, B. Wang, K.S. Shetye, T.J Overbye, J.D. Weber, "Visualization of Large-Scale Electric Grid Oscillation Modes," 50th North American Power Symposium, Fargo, ND, September 2018.

[29] W. Trinh, S. Kunkolienkar, Y. Liu, and T. J. Overbye, "On the Sensitivity of Ring-Down Observed Inter-Area Modes in Large-Scale Electric Grids Using a Simulation Approach," IEEE. Power and Energy Conference at Illinois, Champaign, IL, March 2022

[30] F. Crameri, "Scientific Color Maps", 2018 , Zenodo, http://doi.org/10.5281/zenodo.1243862.

[31] F. Crameri, G.E. Shephard, P.J. Heron, "The Misuse of Color in Science Communication," *Nature Communications*, Vol. 11, pp. 1-10, Oct. 2020.

[32] D. Trudnowski, D. Kosterev, J. Wold, "Open-Loop PDCI Probing Tests for the Western North American Power System," 2014 IEEE PES General Meeting, National Harbor, MD, July 2014.

[33] T.J. Overbye, E.M. Rantanen, S. Judd, "Electric power control center visualizations using geographic data views," Bulk Power System Dynamics and Control 2007 IREP Symp., Charleston, SC, August 2007.

[34] T.J. Overbye, J.L. Wert, K.S. Shetye, F. Safdarian, and A.B. Birchfield, "The Use of Geographic Data Views to Help With Wide-Area Electric Grid Situational Awareness," 2021 IEEE Texas Power and Energy Conference, College Station, TX, Feb. 2021.

[35] J.D. Weber, T.J. Overbye, "Voltage Contours for Power System Visualization," *IEEE Trans. on Power Syst*., vol. 15, pp. 404-409, Feb., 2000.

[36] J.S. Thorp, C.E Seyler, A.G. Phadke, "Electromechanical Wave Propagation in Large Electric Power Systems," *IEEE Trans. Circuits and Systems I*, vol. 45, pp. 614-622, June 1998.

[37] P. Markham, Y. Liu, "Electromechanical Speed Map Development using FNET/GridEye Frequency Measurements," IEEE PES General Meeting, National Harbor, MD, July 2014.

[38] Critical Energy/Electric Infrastructure Information, US Federal Energy Regulatory Commission (FERC); available online at www.ferc.gov/ceii .